128-Gb/s Monolithic Silicon Optical Modulator for Digital Coherent Communication

Tsung-Yang Liow,[1] *Xiaoguang* Tu,[1] *Guo-Qiang* Lo,[1] *Dim-Lee* Kwong,[1]
Kazuhiro Goi,[2] *Akira* Oka,[2] *Hiroyuki* Kusaka,[2] *Yasuhiro* Mashiko,[2] and *Kensuke* Ogawa[2]

Silicon photonic waveguides are promising in small-footprint low-cost monolithic photonic integrated circuits with capability of high-yield mass production using large-diameter wafers. Design, fabrication and performance characterization of a small-footprint monolithic dual-polarization quadrature phase-shift keying silicon-based optical modulator for digital coherent communication, which plays major roles in high-speed optical transport networks, are reported. The monolithic dual-polarization quadrature phase-shift keying silicon optical modulator consists basically of device blocks for quadrature phase-shift keying and a polarization-multiplexing optical circuit, which are monolithically integrated on silicon chip. The polarization-multiplexing optical circuit is based on silicon waveguides which are based on silicon cores and silica clads only, thereby suitable for mass production because the circuit can be fabricated simultaneously with silicon rib waveguides in the blocks for quadrature phase-shift keying. Low-loss monolithic silicon dual-polarization quadrature phase-shift keying optical modulator realized by integration with the polarization-multiplexing optical circuit is shown to have low optical loss. Dual-polarization quadrature phase-shift keying with bit rate as fast as 128 Gb/s is demonstrated based on constellation and bit-error-rate measurements.

1. Introduction

There has been growing data traffic due to wide spreads of broadband local networks, smart phones and mobile tablets. Data from/to the local networks and the wireless equipment are transmitted via optical transport networks consisting of long-reach optical fiber links. This leads to constant growth of network traffic in the trunk optical-fiber links, thereby optical transport networks operated in higher transmission speeds are indispensable. For enhancement of transmission speed in optical transport networks, multi-leveling by increasing bit count per symbol and multiplexing optical signals in different optical states have been adopted as well as increase in symbol rate. Multiple phase-shift keying formats such as QPSK have been exploited to allocating multiple phase states for representation of respective multiple bits. In addition to data multiplication in wavelength divisions by WDM, PDM, in which optical signals are multiplexed in polarization divisions, has been accommodated to optical-fiber transmission.

Digital communications systems have been deployed commercially to permit optical signal transmission at a bit rate as high as 128 Gb/s per wavelength channel in DP-QPSK, which incorporates PDM and QPSK, for signal modulation and coherent phase detection based on optical interference between signal and LO lightwaves for signal demodulation[1)-4)]. The highly multiplexed optical signal modulation of DP-QPSK leads to increased complexity and hence large dimensions of optical transport equipment. Reduction in device footprints and device fabrication costs is, therefore, crucial for commercial deployment of the digital coherent communication systems.

Silicon photonic integrated circuits have the advantage of miniaturization of highly functional photonic circuits because the silicon photonic devices are based on high-index-contrast optical waveguides with silicon cores and silica clads as fundamental building blocks, which allow significant size reduction of photonic circuits into micrometer scales with optical elements such as bend waveguides with a bending radius as small as a few micrometers. Silicon photonic integrated circuits are fabricated by using silicon chip fabrication processes under ceaseless development to accommodate the miniaturization trend of large-scale integration of CMOS circuits. Therefore, silicon photonic integrated circuits are suitable for footprint reduction and monolithic integration as well as high-yield low-cost fabrication using large-diameter SOI wafers.

Optical modulator, which is capable of high-speed optical signal transmission in DP-QPSK format, is one of the key optical devices in digital coherent communication. The commercial deployment of the digital com-

1 Institute of Microelectronics, A*STAR, 11 Science Park Road, Singapore Science Park II, Singapore
2 Silicon Technology Department

Panel 1. Abbreviations, Acronyms, and Terms.

QPSK—Quadrature Phase-Shift Keying
Signal modulation format in multi-level phase-shift keying using orthogonal quadrature components to accommodate two bits per symbol.

DP-QPSK—Dual-Polarization Quadrature Phase-Shift Keying
Signal multiplication and modulation format used in digital coherent communication, in which QPSK signals are multiplexed in two orthogonal linear polarization states.

WDM—Wavelength Division Multiplexing
Signal multiplication scheme, in which optical signals are alocated into wavelength-division slots.

PDM—Polarization-Division Multiplexing
Signal multiplication by allocating plural polarization states to accommodate optical signals.

I—In-Phase
Phase state of a bit, which is specified as a point on circumference crossing the real axis in two-dimensional polar representation.

Q—Quadrature
Phase state of a bit, which is specified as a point on circumference crossing the imaginary axis in two-dimensional polar representation.

LO—Local Oscillator
Local light source of which lightwave is superposed to signal lightwave to produce optical interference for phase detection in a coherent optical receiver.

RF—Radio Frequency
Radio frequency or high frequency of electromagnetic wave.

TE polarization—Transverse-Electric Polarization
State of linear polarization with its electric field parallel to planar substrate plane, on which optical circuits are formed.

TM polarization—Transverse-Magnetic Polarization
State of linear polarization with its magnetic field parallel to planar substrate plane, on which optical circuits are formed.

SOI wafer—Silicon-on-Insulator Wafer
A type of silicon wafer, on which thin silicon single crystal (SOI) layer is disposed on an insulator of burried oxide (BOX) layer and the BOX layer is disposed on a silicon planar substrate.

TO effect—Thermo-Optic Effect
Effect that refractive index depends on and changes with temperature in semiconductor or insulator.

carrier-plasma dispersion—Carrier-Plasma Dispersion
Effect that refractive index depends on and changes with carrier concentration due to free-carrier absorption in semiconductor.

PRBS—Pseudo-Random Bit Stream

BER—Bit Error Rate

OSNR—Optical Singal-to-Noise ratio

VOA—Variable Optical Attenuator

EDFA—Erbium-Doped Fiber Amplifier

BPF—Band Pass Filter

munication systems will be leveraged by realization of small-footprint low-cost monolithic silicon optical modulator for 128-Gb/s DP-QPSK transmission.

High-speed silicon optical modulators have been developed for optical-fiber telecommunications to achieve long-haul transmission performance comparable with that of commercialized lithium niobate (LN) optical modulators and to realize small-footprint low-loss monolithic silicon optical modulator operated in 64-Gb/s QPSK[5)6)]. Monolithic silicon DP-QPSK modulator is reported in this paper, which has been developed for 128-Gb/s digital coherent communication.

2. Monolithic silicon DP-QPSK optical modulator

2.1 Overview of monolithic silicon DP-QPSK optical modulator

Two orthogonal components of QPSK signals are generated and multiplexed in orthogonal linear polarization states in DP-QPSK optical modulator. Monolithic silicon DP-QPSK optical modulator is designed and fabricated using two QPSK optical modulators and a PDM optical circuit as elemental building blocks based on silicon high-index-contrast optical waveguides. Small-footprint silicon DP-QPSK modulator is realized by monolithic integration of these blocks on SOI wafer of 20-cm diameter.

Layout of monolithic silicon DP-QPSK optical modulator and scheme of modulation signals in DP-QPSK format are illustrated in Fig. 1 and elaborated below. Continuous-wave (CW) single-wavelength light from a laser source is input to a Si DP-QPSK optical modulator. The input light is split and guided to two paths with equal power ratio. Two QPSK modulators (QPSK1, QPSK2) are inserted in the two paths, respectively. Each QPSK modulator consists of a nested Mach-Zehnder (MZ) interferometer as illustrated in Fig. 1[6)]. The nested MZ interferometer, which includes a pair of sub MZ interferometers generating phase

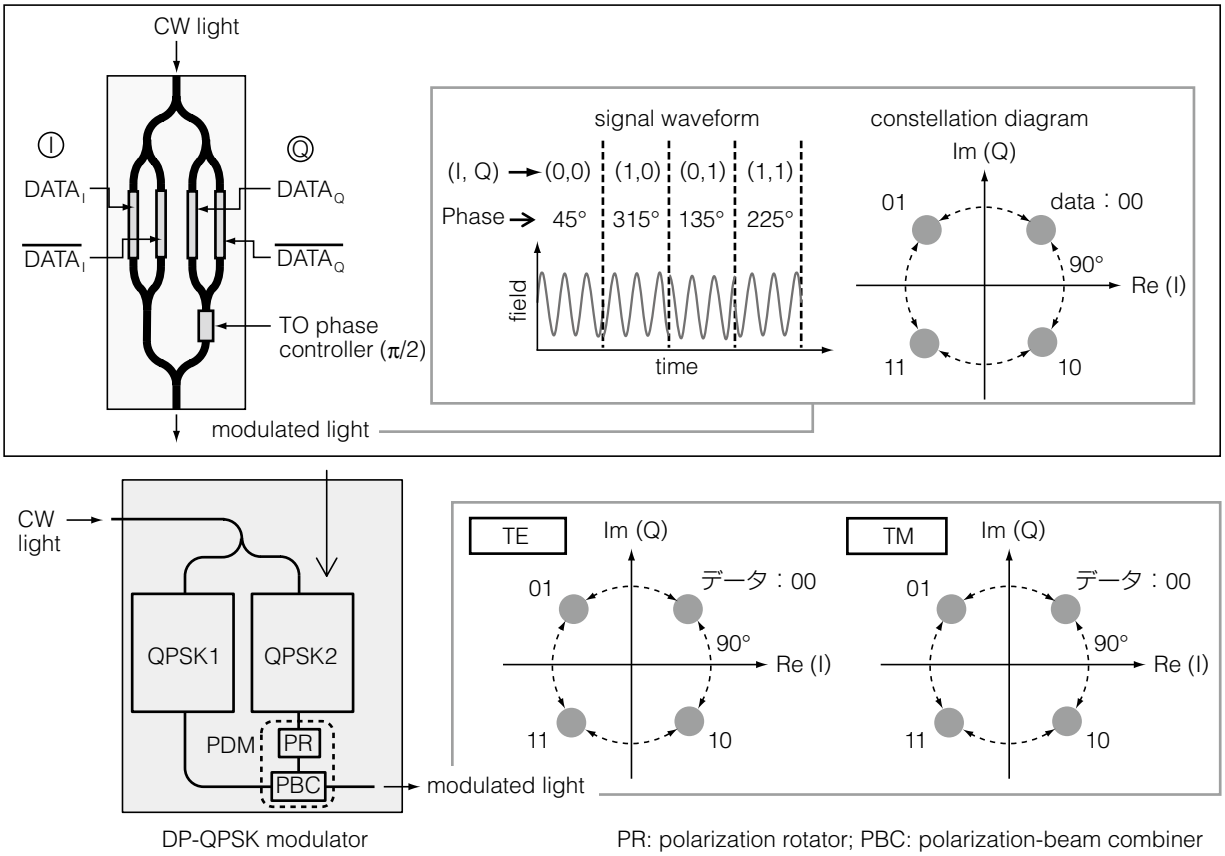

Fig. 1. Layout of silicon DP-QPSK modulator and scheme of DP-QPSK signals.

modulation signals in I and Q components, respectively, is made of silicon high-index-contrast waveguides. The sub MZ interferometer is a single MZ waveguide consisting of an input waveguide split into two waveguides forming two MZ arms, in-line rib-waveguide phase shifters in the MZ arms for high-speed phase modulation and an output waveguide to which the two waveguides are recombined. Modulated lights from the two QPSK modulators are both in TE polarization because the Si-based nested MZ interferometer operates only in TE polarization. The modulated light from QPSK2 is rotated 90-degree into TM polarization through a polarization rotator (PR) and combined with the other modulator light from QPSK1 in a polarization-beam combiner (PBC). Two components of QPSK signals in orthogonal linear polarization states are thus generated to form DP-QPSK signals. The PDM optical circuit consists of PR and PBC based on integrated high-index-contrast silicon waveguides.

Digital coherent system, to which a silicon DP-QPSK modulator is introduced, is schematically illustrated in Fig. 2. Optical signals after single-mode optical-fiber transmission line are split in X and Y polarization states. The optical signals are combined with LO light to generate optical interference signals in respective polarization states for coherent phase detection at QPSK receivers, and demodulated as QPSK signals at a digital signal processor (DSP)[2].

QPSK signals are generated in QPSK modulators by phase modulation of I and Q components in sub MZ interferometers. QPSK signals are illustrated in Fig. 1[6][7]. Optical signals are assigned as respective four phase states, which are equally separated 90 degree ($\pi/2$) from adjacent phase states in signal coding in QPSK format. Optical phase is modulated per symbol as depicted in a signal waveform in Fig. 1. Symbol is defined as a group of signals coded in a time slot with a unit of baud. Two bits are coded per symbol in QPSK. The four phase states are represented in a constellation diagram in Fig. 1 as four spots equally spaced on a circumference centered on the origin of two-dimensional Cartesian coordinates. I and Q components are assigned as real (Re) and imaginary (Im) axes on the two-dimensional complex plane. A phase difference of $\pi/2$ is required between carrier lightwaves in I and Q components, respectively. A phase controller using TO effect is inserted to generate and sustain $\pi/2$ phase difference[5]. To suppress signal deterioration due to spectral broadening and frequency chirping, each sub MZ interferometer is operated in push-pull mode, where RF electrical signals of opposite polarities (DATA and inverted DATA) are applied to respective arms of the sub MZ interferometer as input electrical signals from electrical signal drivers[8][9].

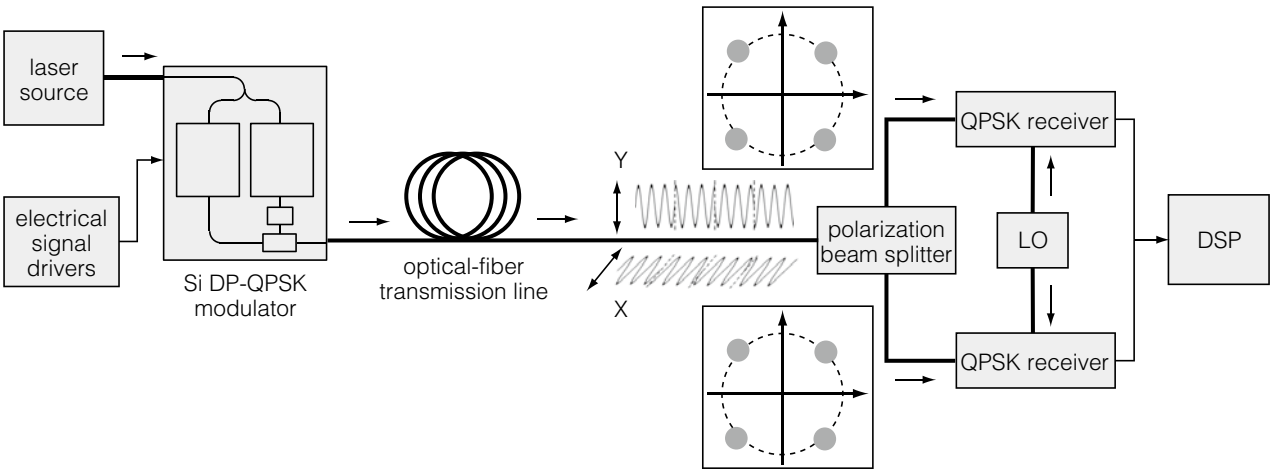

Fig. 2. Schematic diagram of digital coherent communication system.

2.2 Design and fabrication of monolithic silicon DP-QPSK optical modulator

Monolithic silicon DP-QPSK modulator was fabricated on SOI wafer of 20-cm diameter by 130-nm node CMOS fabrication processes. A top-view photograph of a fabricated monolithic Si DP-QPSK modulator on a SOI chip is presented in Fig. 3 with waveguide layout of the modulator. Two QPSK modulators and a PDM optical circuit were integrated with germanium photodetectors (PDs) in a footprint as small as 6.5x5.1 mm^2, which is about 1/10 in comparison with a footprint of commercialized LN QPSK modulators incorporated with discrete free-space PDM optics[10]. Ge PDs are used for monitoring modulated lights to sustain $\pi/2$ phase difference between I and Q components in each sub MZ interferometer.

Phase shifter in each arm of sub MZ interferometer is operated in 32 Gbaud for 128-Gb/s DP-QPSK operation. Attenuation of RF signals to phase shifter on modulator chip is an issue in such high-speed operation. Straight traveling-wave electrodes without any bends were employed to eliminate RF power attenuation. Input contact metal pads connected to the straight traveling-wave electrodes were disposed on an edge of the modulator chip as shown in the top-view photograph in Fig. 3 in a configuration similar to 64-Gb/s Si QPSK modulator[6][7]. The contact metal pads for RF signal termination were disposed on the opposite edge with extended traveling-wave electrodes aligned beside germanium PDs. RF attenuation in the extended part of the traveling-wave electrodes is not relevant as this occurs after RF propagation through the phase shifters. The traveling-wave electrodes and the contact pads were made of aluminum deposited in 2-μm thickness.

To avoid input and output optical fibers interfering with the RF bonding wires, input and output mode-field converters consisting of inverted taper Si waveguides were located on side facets (90 degree angle to the RF input/output facets) using high-index-contrast Si channel waveguide bends of 25-μm bending radius as shown in Fig. 3. Increase in footprint due to the waveguide bends is less than 10% of the footprint of QPSK modulators. Optical loss due to the waveguide bends is as low as 0.04 dB per semicircle.

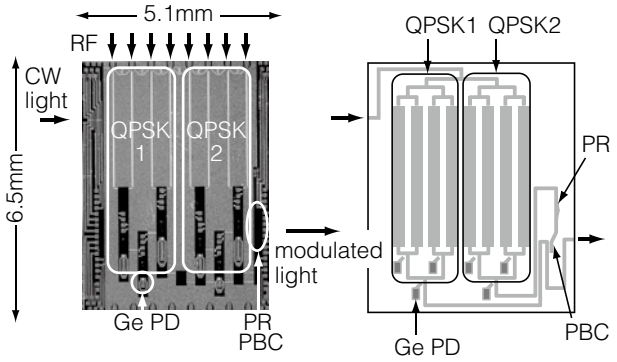

Fig. 3. Top-view photo and waveguide layout of monolithic silicon DP-QPSK modulator.

2.3 High-speed silicon phase shifter

High-speed phase modulation in silicon rib-waveguide phase shifters in Si DP-QPSK modulator was achieved by using the mechanism of carrier-plasma dispersion as used for Si QPSK modulator[6][11][12]. In the carrier-plasma dispersion, silicon refractive index increases with decreasing free-carrier concentration in silicon, while decreases with increasing free-carrier concentration. Phase modulation due to refractive index modulation in rib-waveguide phase shifters was achieved with RF application to lateral PN junction formed in the rib-waveguide phase shifters. 32-Gbaud phase modulation is possible for carrier depletion under DC reverse bias, because of fast displacement of free carriers with high drift velocity under the reverse bias[13][14].

Silicon rib-waveguide phase shifter connected with traveling-wave electrodes has a cross-section illustrated in Fig. 4. Rib-waveguide core of 500-nm rib width and 220-nm rib height was formed in SOI layer on SOI wafer. Silicon slab layers adjacent to the central rib on the both sides have a height of 95 nm. The core was embedded between top and bottom clads. Lateral PN junction was formed in the middle of the rib core. The lateral PN junction is suitable to high-yield fabrication, because the junction was formed only by ion implantation without any deposition or epitaxy of additional doped layers[15]. Traveling-wave electrodes were connected on the top of side slab regions, where doping concentration was increased (P+ and N+ regions) for lower electrical contact resistance. Coplanar waveguides were employed as the traveling-wave electrodes. Coplanar waveguide is capable of high isolation of RF signals with wide ground planes, thereby cross-talk between RF signals applied to each MZ arms is suppressed efficiently.

2.4 Optical circuit for polarization-division multiplexing

PDM optical circuit consists of a polarization rotator (PR) and a polarization-beam combiner (PBC), to which the polarization rotator is connected, as illustration and schematic layout in Fig. 5. Optical signals emitted in TE polarization from QPSK1 are propagated through waveguide 1 (WG1) and the PBC and then emitted out of the DP-QPSK modulator. Optical signals in TE polarization from QPSK2 are propagated through waveguide 2 (WG2), transformed into TM-polarized optical signals via 90-degreee polarization rotation in PR, transferred to WG1 and finally emitted out of the DP-QPSK modulator. TE and TM polarization states correspond to X and Y polarization states in optical receiver side in this study.

The PR, which consists of a silicon partial rib waveguide, was designed to yield gradual change in its cross-section according to light propagation along the waveguide so that effective refractive indices of the fundamental guided modes in TE and TM polarization states change adiabatically along light propagation direction and are finally reversed in their magnitudes, thereby low-loss polarization rotation was achieved[16]. The PBC, which consists of directionally coupled waveguides, allow spatial transfer from WG2 to WG1 only for the TM guided mode on account of a difference in direction coupling constant between the TE and TM guided modes. The PR and the PBC were formed with 220-nm silicon core embedded between the silica top and bottom clads on the basis of common design rules with the rib-waveguide phase shifter. The PDM optical circuit was, therefore, fabricated in simultaneously with the rib-waveguide phase shifters, and is suitable for high-yield low-cost fabrication.

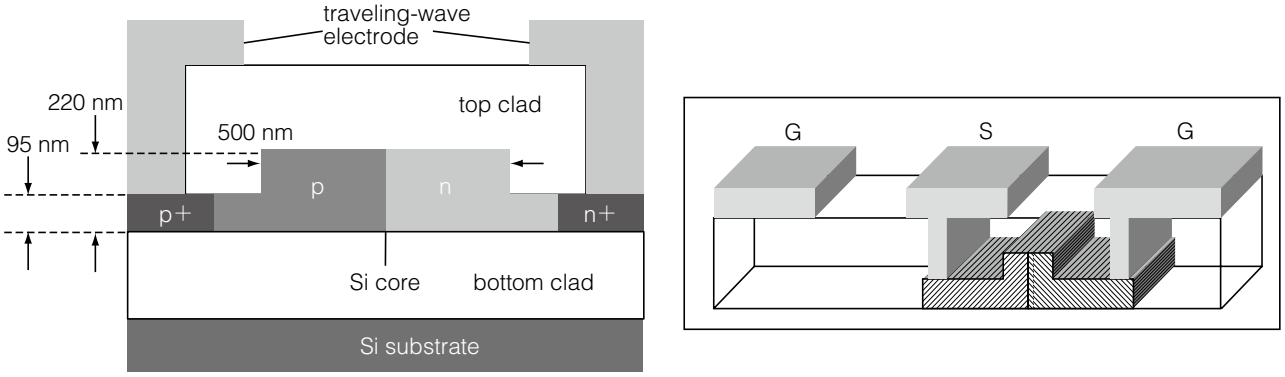

Fig. 4. Cross-section of traveling-wave silicon rib-waveguide phase shifter.

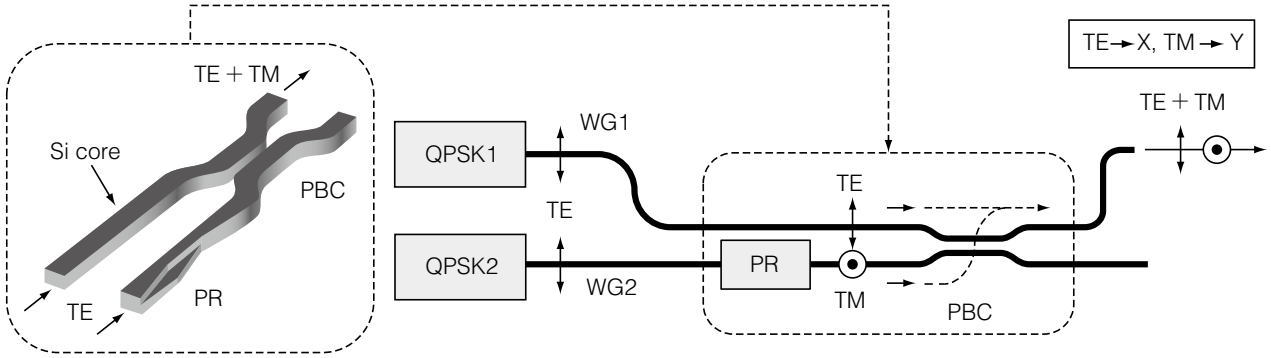

Fig. 5. Silicon PDM optical circuit.

3. Characteristics of monolithic silicon DP-QPSK optical modulator

3.1 Characteristics of polarization-division multiplexing

Low-loss 128-Gb/s monolithic silicon DP-QPSK modulator has been realized with low-loss silicon PDM optical circuit, because low-loss 64-Gb/s QPSK modulator was already completed[6)7)]. Transmission optical spectra of the silicon PDM optical circuit described in the previous section are plotted in a wavelength range of C band in Fig. 6. The spectra were acquired by using a discrete PDM optical circuit for testing. Transmittance of TE-polarized light from QPSK1 (TE①→TE①) is higher than -1 dB. Transmittance of TM-polarized light from QPSK2 (TE②→TM②)after the polarization rotation and transfer from WG2 to WG1 is higher than -3 dB.

Insertion loss spectra of a monolithic silicon DP-QPSK modulator, in which a PDM optical circuit and modulators QPSK1 and QPSK2 were integrated, are plotted in Fig. 7. Insertion loss associated with TE or TM component was acquired by holding respective one of the two modulators in off state to shut off undesired output light with adjustment of TO $\pi/2$ phase controllers. Insertion loss associated with each polarization state is lower than 17 dB. Insertion loss with both of TE and TM components is lower than 13 dB. The insertion loss is lower than reported for other monolithic silicon DP-QPSK modulators, and low-loss monolithic silicon DP-QPSK modulator is realized[17)].

3.2 128-Gb/s DP-QPSK

128-Gb/s DP-QPSK operation has been confirmed in constellation and BER measurements in back-to-back configuration with the set-up depicted in Fig. 8. Electrical signals in PRBS at a symbol rate of 32 Gbaud were input to a monolithic silicon DP-QPSK modulator. Light from a laser source was split to input light to the modulator and LO light for coherent detection in X and Y polarization states. Constellation diagrams were acquired by using a high-speed oscilloscope equipped with an off-line digital signal processor for signal demodulation. A BER tester was used for BER measurements. In the BER measurements, power of the modu-

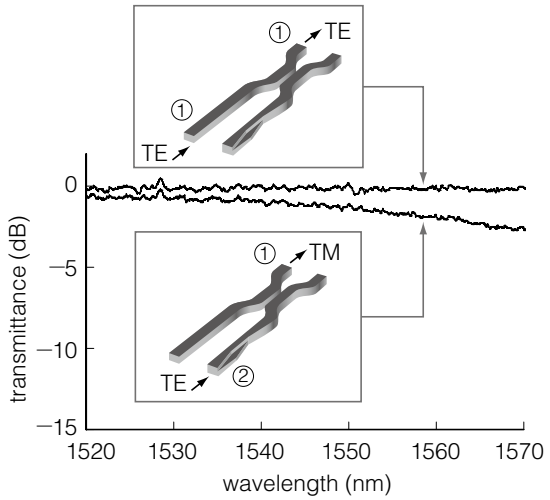

Fig. 6. Transmission spectra of silicon PDM optical circuit.

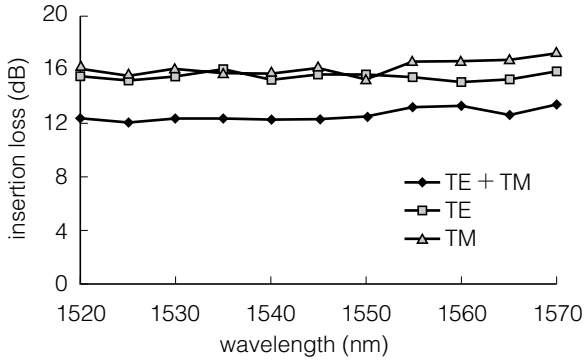

Fig. 7. Insertion loss spectra of silicon DP-QPSK optical modulator.

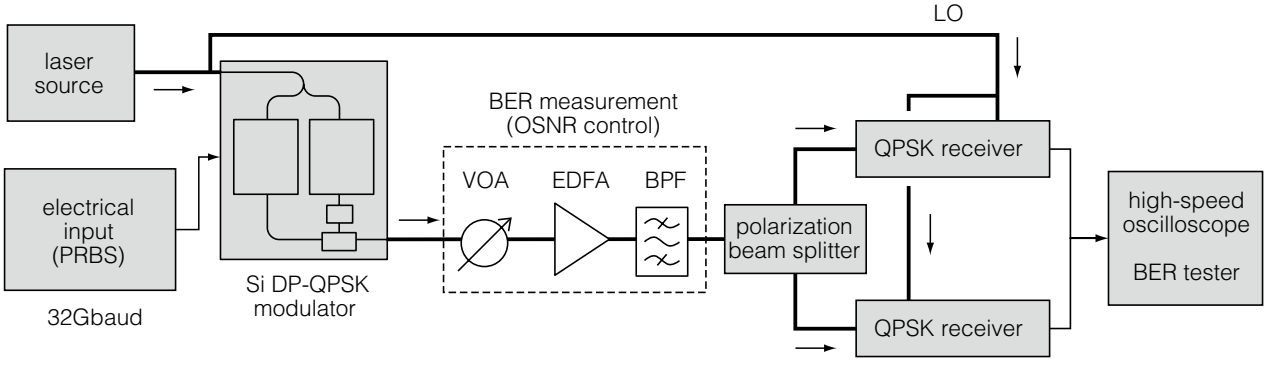

Fig. 8. Block diagram of constellation and BER measurements.

lated light was adjusted by a VOA to control OSNR at specified levels. Amplified spontaneous emission from an EDFA was a source of optical noise. Spectral bandwidth was 0.1 nm after a BPF.

Measured back-to-back constellation diagrams in X and Y polarization states are presented with a schematic constellation diagram in Fig. 9. Four constellation spots are clearly observed in the X and Y constellation diagrams as QPSK bits illustrated in the schematic diagram with a BER of 10^{-6}. 128-Gb/s DP-QPSK implies that a high-performance soft-decision forward-error-correction (FEC) algorithm, which requires 20% margin accommodating error-correction codes in total transmission bits, can be incorporated to 100-Gb/s data transmission with a FEC margin sufficient for error-free digital coherent communication systems[4]. DP-QPSK operation was reported for other silicon modulators at a bit rate of 112 Gb/s[17][18].

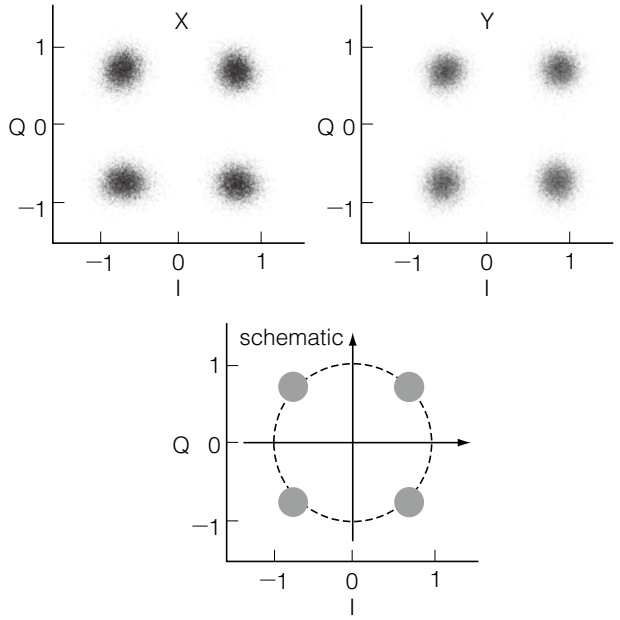

Fig. 9. Constellation diagrams obtained in X and Y polarization states and a schematic diagram for reference.

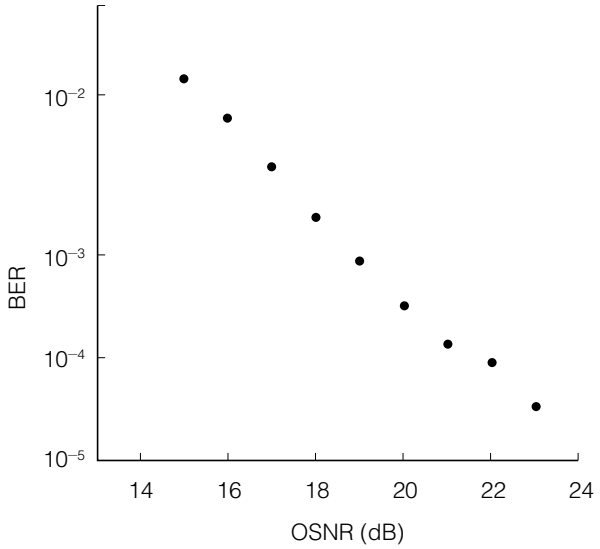

Fig. 10. BER characteristics.

BER data in Fig. 10 shows a good characteristic with no noise floor. At the upper BER limit of 10^{-2} for error-free operation with the FEC algorithm, OSNR is obtained as about 15 dB from the BER characteristics in Fig. 10, thereby digital coherent communication based on error-free DP-QPSK is possible at OSNR ≧ 15 dB by using the monolithic silicon DP-QPSK modulator studied in this paper.

4. Conclusion

Monolithic silicon MZ modulator has been described in the lights of modulator layout and performance for operation in DP-QPSK format. Low-loss monolithic silicon DP-QPSK modulator has been realized with a monolithically integrated low-loss silicon PDM optical circuit. DP-QPSK operation has been confirmed in constellation and BER measurements at a bit rate as high as 128 Gb/s. For application to digital coherent communication systems, error-free 128-Gb/s DP-QPSK operation has been proved at OSNR ≧ 15 dB.

References

1) Y. Miyamoto and I. Morita: "High-capacity Optical Communication System Enhanced by Digital Signal Processing Technologies," J. IEICE vol.94, no.2, pp.72-78, 2011.
2) K. Kikuchi: "Coherent Transmission Systems," 34th European Conference and Exhibition on Optical Communication (IEEE, Piscataway, 2008) Th.2.A.1.
3) P. J. Winzer and R. J. Essiambre : "Advanced Modulation Formats for High-Capacity Optical Transport Networks," J. Lightwave Technol., vol.24, no.12 , pp.4711–4728, 2006.
4) K. Onohara, et al.: "Soft decision FEC for 100G transport systems," in Optical Fiber Communication Conference and Exposition (OFC) and National Fiber Optic Engineers Conference (NFOEC) (Optical Society of America, Washington, DC, 2010) OThL1.
5) K. Goi, et al.: "11-Gb/s 80-km Transmission Performance of Zero-Chirp Silicon Mach-Zehnder Modulator," Opt. Exp. vol.20, no.26, pp.B350-B356, 2012.
6) K. Goi, et al.: "DQPSK/QPSK Modulation at 40-60 Gb/s using Low-Loss Nested Silicon Mach-Zehnder Modulator," in Optical Fiber Communication Conference and Exposition (OFC) and National Fiber Optic Engineers Conference (NFOEC) (Optical Society of America, Washington, DC, 2013), OW4J.4.
7) T.-Y. Liow, X. Tu, G.-Q. Lo, D.-L. Kwong, K. Goi, A. Oka, H. Kusaka, and K. Ogawa: "Silicon Quadrature Phase-shift-keying Modulator for 40- and 100-Gb/s Transmission," Fujikura Technical Review, vol.43, pp.1-5, March, 2014.

8) F. Koyama and K. Iga: “Frequency Chirping in External Modulators,” J. Lightwave Technol. vol.6, pp.87-93, 1988.
9) A. H. Gnauck and P. J. Winzer: “Optical Phase-Shift-Keyed Transmission,” J. Lightwave Technol. vol.23, pp.115-130, 2005.
10) H. Kusaka, et al.: “Monolithic Photonic Integrated Circuit for Optical Performance Monitoring of Silicon Mach-Zehnder Modulator in C and L Bands,” in 18th OptoElectronics and Communications Conference / Photonics in Switching 2013 (IEICE, Kyoto, 2013), MM1-4.
11) O. Mikami and H. Nakagome: “Waveguided Optical Switch in InGaAs/InP using Free-Carrier Plasma Dispersion,” Electron. Lett. vol.20, no.6, pp. 228-229, 1984.
12) R. A. Soref and B. R. Bennet : “Electrooptical Effects in Silicon,” J. Quantum Electron., vol.23, no.1, pp.123-129, 1987
13) F. Y. Gardes, et al., “A Sub-Micron Depletion-Type Photonic Modulator in Silicon on Insulator,” Opt. Exp. vol.13, no.22, pp.8845-8854, 2005.
14) K. Ogawa et al.: “Low-Loss High-Speed Silicon Mach-Zehnder Modulator for Optical-Fiber Telecommunications,” Proc. SPIE vol.8629, pp.86290U-1-86290U-8, 2013.
15) T.-Y. Liow, K.-W. Ang, Q. Fang, J.-F. Song, Y.-Z. Xiong, M.-B. Yu, G.-Q. Lo, and D.-L. Kwong, “Silicon Modulators and Germanium Photodetectors on SOI: Monolithic Integration, Compatibility, and Performance Optimization,” IEEE J. Sel. Top. Quantum Electron. vol.16, no.1, pp.307-315, 2010.
16) K. Goi, et al.: “Low-Loss Silicon Partial-Rib Waveguide Polarization Rotator,” in 18th Microoptics Conference (Tokyo, 2013) F6.
17) P. Dong, C. Xie, L. Chen, L. L. Buhl, and Y.-K. Chen: “112-Gb/s Monolithic PDM-QPSK Modulator in Silicon,” Optics Express vol.20, no.26, pp.B624-B629, 2012.
18) B. Milivojevic, et al.: “112Gb/s DP-QPSK Transmission Over 2427km SSMF Using Small-Size Silicon Photonic IQ Modulator and Low-Power CMOS Driver,” in Optical Fiber Communication Conference and Exposition (OFC) and National Fiber Optic Engineers Conference (NFOEC) (Optical Society of America, Washington, DC, 2013), OTh1D.1.